Journal of Geodetic Science

• 3(1) • 2013 • 32-39 DOI: 10.2478/jogs-2013-0004 •

Examination of two major approximations used in the scalar airborne gravimetric system — a case study based on the LCR system

Research Article

X. Li*

ERT at NOAA's NGS, 1315 East-West Highway, Silver Spring, Maryland, 20910, U.S.A.

Abstract:

Airborne gravimetry has been proved to be the primary technique to efficiently obtain middle to short wavelength signals of the Earth's gravity field in regional geodetic applications. In particular, the LCR (LaCoste & Romberg) based scalar system (i.e., only measuring the vertical component of the gravity) is widely used or still in use for regional geoid improvements. In various aspects, many previous publications have shown positive contributions from the airborne gravity data obtained from such a system. However, the system equation used in these publications has several unnecessary or unclear approximations. By using the exact formulas and realistic data sets, the numerical analysis in this paper clearly shows that: 1) the higher order terms in the Eötvös correction neglected by Harlan (1968) are rather small (in μGal level), but are systematic mainly depending on latitude and height; 2) neglecting the roll and pitch angles can cause up to hundreds of mGal errors in the raw (unfiltered) gravity measurements if the lever-arm is not set up appropriately; 3) large (200s) smoothing windows have to be applied to reduce the lever-arm noise into sub-mGal level; 4) even under strong lever-arm setup conditions, i.e., no "horizontal offset" between the GPS antenna and the gravimeter, accurate (10 arc-minute ∼ 5 arc-minute) attitude angles from IMU (Inertial Measurement Units) are required to keep the lever-arm noise in sub-mGal level in the raw observables.

Keywords:

Eötvös Correction • Inertial Measurement Units • Lever-arm Correction • Scalar Airborne Gravimetry

Received 24-10-2012; accepted 22-01-2013

1. Introduction

As a physical variable that is closely related to the mass distribution of the Earth, gravity is very helpful to geodesists and geophysicists in determining the figure of the Earth and understanding its subsurface structure (Heiskanen and Moritz 1967, Wahr 1996). For instance, in geodesy, gravity is needed almost everywhere, because only this quantity offers the spatial orientation of the local horizon plane (Wahr 1996). Many methods such as SST (satellite-to-satellite tracking, Rummel 1979), SGG (satellite gravity gradiometry, Rummel 1979), INS/GPS vector gravimetry (Jekeli 2000, Kwon and Jekeli 2001), and airborne scalar gravimetry (Brozena et al. 1988, Forsberg et al. 2001) have been developed for gravity field determination over the decades.

The satellite missions are mainly designed to obtain medium to long (∼>50 km) wavelength gravity field information, while the other moving base gravimetric systems are used for detecting the medium to short (∼<50 km) wavelength contribution. For instance, in the scalar system, Olesen (2003) reported a spatial resolution of 6km or even better with 1∼2 mGal accuracy. A relatively recent study (Li and Jekeli 2008) in the vector system obtained about 2km spatial resolution with 1∼3 mGal precision and as good as sub-mGal (0.64 mGal) repeatability. SGL (Sander Geophysics Limited) showed even better resolution and accuracies (30 0m with RMS=0.4 mGal; Sander et al., 2011) in their unique AIRGrav (Airborne Inertially Referenced Gravimeter) system, which is based on a customized gyroscopically stabilized platform, when operating

*E-mail: Xiaopeng.Li@noaa.gov, Tel.: +1(301)713-3202x210

VERSITA

in a slow speed (∼16 m/s). Note: these sub-km spatial resolution and sub-mGal accuracy from SGL were not along the survey lines as it is customary. They were the grid resolution and grid accuracy, which were based on 1.25 km frequency domain spatial low pass of the 20-second filtered line data that were 50 to 100 meters apart to each other (Sander and Ferguson, 2010). However, Studinger et al. (2008) indeed showed in a case study that the AIRGrav system is superior to the LCR system in terms of resolution and accuracy.

Beside the mechanical differences of these two systems, where geodesists have limited power to control, the equations in the scalar systems have several ambiguous issues that need to be cleared when compared with the equations used in the 3D cases, for instance as derived by Jekeli (2000). At present, the scalar airborne equations used in most of cases ignore the higher order terms in the Eötvös term and have a fuzzy positioning transformation from the phase center of the GPS antenna to the gravimeter's mass center. Several groups, such as Laboratoire de Géphysique at Université Montpellier (Verdun 2000), and LAboratoire de Recherche en Géodésie, Institut Géographique National France (de Saint-Jean et al 2007) among others, tried to analyze these problems in some case studies, and found that these approximations can be 'safely' neglected in their applications. By both rigorous yet succinct derivations and extensive numerical evaluations, this study confirms the magnitudes of these approximation effects are indeed small in the context of the current airborne survey accuracies, i.e., mGal level, especially after filtering, smoothing or denoising processes. However, these approximations need to be removed for the theoretical completeness and for the future high accuracy systems, μGal level. The rest of this paper is organized as follows. By using both simulated and real flight data, section 2 examines the approximations made by Harlan (1968) in computing the Eötvös correction. With the accurate attitude information provided by the on-board IMU, the lever-arm effects are also studied based on both simulated and real data in Section 3. From the analytical developments and the numerical tests, some conclusions are given in Section 4.

2. The analysis of the Eötvös correction

Unlike the equations of vector gravimetry (Jekeli 2000) that solves the full gravity vector, the scalar system (Brozena and Peters 1988, Forsberg et al. 2001, and Olesen 2003, among others) only computes the vertical gravity component. Usually, they are solved in the local navigation frame (Jekeli 2000), which requires the computation of the Eötvös correction that is the gravity changes due to the change in the centrifugal acceleration induced by the horizontal velocities of the reference frame. Even though the closed form equation for this computation had been published for many years, for instance see last page in Jekeli (2000), interestingly, some researchers are still using the approximated version developed by Harlan (1968), where higher order (O^2) terms of the Earth's flattening were omitted. The total neglecting error is the difference between Eq. (4) and Eq. (13) in Harlan (1968) (for the reader's convenience, these two equations are listed again in appendix A as Eq. (A1) and Eq. (A2), respectively). Based on these approximations, Harlan (1968) gave the following Eötvös correction as shown in Eq. (1).

$$E = \frac{V_N^2}{a}\left[1 - \frac{h}{a} + f\left(2 - 3\sin^2\phi\right)\right] + \frac{V_E^2}{a}\left[1 - \frac{h}{a} - f\sin^2\phi\right] + 2V_E\omega_e\cos\phi, \quad (1)$$

where a and f are the semi-major axis and the flattening of the reference ellipsoid; h is the ellipsoid height; ϕ is the geodetic latitude; V_N and V_E are the north and east velocities; and ω_e is the Earth's angular rotation rate.

If the same velocity information is used, Eq. (1) is basically the first order approximation of the closed formula as shown in Eq. (2) after we work out the following partial derivatives as shown in Eqs (3)-(6) (The basic evaluation of the Taylor series are left for interested readers):

$$E = \frac{V_N^2}{\frac{a(1-(2f-f^2))}{\left[1-(2f-f^2)\sin^2\phi\right]^{3/2}} + h} + \frac{V_E^2}{\frac{a}{\left[1-(2f-f^2)\sin^2\phi\right]^{1/2}} + h} + 2V_E\omega_e\cos\phi, \quad (2)$$

$$\frac{\partial}{\partial h}\left\{\frac{1}{\frac{a(1-(2f-f^2))}{\left[1-(2f-f^2)\sin^2\phi\right]^{3/2}} + h}\right\}_{h=0;f=0} = -\frac{1}{\left[\frac{a(1-(2f-f^2))}{A^{3/2}} + h\right]^2}_{h=0;f=0} = -\frac{1}{a^2}, \quad (3)$$

$$\frac{\partial}{\partial f}\left\{\frac{1}{\frac{a(1-(2f-f^2))}{\left[1-(2f-f^2)\sin^2\phi\right]^{3/2}} + h}\right\}_{h=0;f=0} = -\frac{\frac{a(-2+2f)}{A^{3/2}} + 3/2\frac{a(1-2f+f^2)(2-2f)\sin^2\phi}{A^{5/2}}}{\left[\frac{a(1-(2f-f^2))}{A^{3/2}} + h\right]^2}_{h=0;f=0} = \frac{2-3\sin^2\phi}{a}, \quad (4)$$

$$\frac{\partial}{\partial h}\left\{\frac{1}{\frac{a}{\left[1-(2f-f^2)\sin^2\phi\right]^{1/2}} + h}\right\}_{h=0;f=0} = -\frac{1}{\left[\frac{a}{A^{1/2}} + h\right]^2}_{h=0;f=0} = -\frac{1}{a^2}, \quad (5)$$

$$\frac{\partial}{\partial f}\left\{\frac{1}{\frac{a}{\left[1-(2f-f^2)\sin^2\phi\right]^{1/2}}+h}\right\}_{h=0;f=0} = -1/2\frac{a(2-2f)\sin^2\phi}{\left[\frac{a}{A^{1/2}}+h\right]^2 A^{3/2}}_{h=0;f=0} = -\frac{\sin^2\phi}{a}, \quad (6)$$

where $A := 1-(2f-f^2)\sin^2\phi$

Harlan (1968) only mentioned that the magnitude of the second order term is small (<0.03mGal at mid-latitude) without investigating the nature of it in real cases. Three typical real flight data sets (see Fig. 1) are selected from the Alabama survey campaign conducted by the National Geodetic Survey as a part of its GRAV-D (Smith, 2007) project to test all the neglecting effects. The total approximation errors along each of the selected flights are shown by the thick solid lines in Fig. 2; all referring to the red axes. The velocity information ($V_E^2+V_N^2$) of each flight is also plotted in the same figure by using the thin dotted line with the same color as the color for the corresponding errors, but is referring to the black y-axis on the right. Fig. 2 shows that the approximation errors are basically proportional to the velocity information because of the multiplication of the velocity squares in Eq. (1).

Instead of directly plotting the errors, Fig. 3 shows the approximation errors on the coefficients of V_N^2 and V_E^2 in Eq. (1), i.e, $\frac{1}{\frac{a(1-(2f-f^2))}{\left[1-(2f-f^2)\sin^2\phi\right]^{3/2}}+h}-\frac{1}{a}\left[1-\frac{h}{a}+f\left(2-3\sin^2\phi\right)\right]$ and $\frac{1}{\frac{a}{\left[1-(2f-f^2)\sin^2\phi\right]^{1/2}}+h}-\frac{1}{a}\left[1-\frac{h}{a}-f\sin^2\phi\right]$. The takings off and landing periods clearly show that the amplitudes grow with respect to the height changes. The trend in the business part, when the aircraft was flying in the north-south direction, basically tells that the approximation errors are also latitude-dependent. To verify this, Flight A is shifted 20^o to 40^o north by a step of 5^o, where the ellipsoid heights and longitudes are remaining the same. The corresponding coefficient errors along these simulated flights are shown in Fig. 4. The latitude depended biases are shown clearly at the beginning and the end of the lines where the "aircraft" are supposed to be stationary with respect to the Earth. Furthermore, the V_N^2 coefficient bias is more sensitive to the latitude than the counterparts for V_E^2. The intersections of the colored lines for the same type of coefficient errors in Fig. 4 also remind us that the effects is a combination of the latitude and height, which makes the errors in higher latitudes having a larger amplitude than the one in lower latitudes.

From the above analysis, we see that the total approximation error, which includes not only the second order term but also all higher order terms, is generally at the μGal level. However, it shows a systematic characteristic related to latitude and height in a complicated way, which cannot be easily removed once the approximate equation is employed. Even though the magnitude is indeed very small in the context of the current airborne instrument's accuracy, no approximate formula should be used in order to avoid these systematic effects, especially considering the fact that the closed formula is not very difficult to be implemented with today's computation power.

3. The analysis of the lever-arm effect

Due to the physical limitations in airborne surveying, the position of the GPS antenna cannot coincide exactly with the position of the gravimeter. As a result, the GPS positioning solution needs to be transformed into the gravimeter's position. Thus, the lever-arm correction (Jekeli 2000, Li 2007, de Saint-Jean et al 2007, Melachroinos et al 2010) has to be applied to account for the position difference between the GPS antenna and the gravimeter, $\vec{b} = [\Delta x, \Delta y, \Delta z]^T$ as shown in Fig. 5. In the 3D cases, this can be done rigorously by using all the attitude angles provided by the IMU; see Li (2011a,b) for the details. However, for the scalar system based on the LCR system (Valliant 1992 among other similar manuscripts), the lever-arm correction is a gray area in some previous publications, where not too much information was given. Olesen (2003) found in a case study that the RMS value of the filtered lever-arm effect was 0.4 mGal when the "horizontal" component of the lever-arm is 7.2 m, and concluded that for "horizontal" offsets less than 1 meter, the effect can safely be neglected.

Based on a set of real pitch and roll angles (as shown in Fig. 6 and Fig. 7) that were provided by the on board IMU during a typical airborne flight, the lever-arm effects on the vertical accelerations at various scenarios are computed. For instance, Fig. 8 shows the effect corresponding to the case of $[\Delta x = 1\ \text{m}, \Delta y = 1\ \text{m}, \Delta z = 1\ \text{m}]^T$ with both the roll and pitch in presence. From the figure, we see that the magnitude of these errors are normally from 100 mGals to 200 mGals; the extreme values can be larger than half thousand mGals; the RMS is about 100 mGals. By altering the appearance of the attitude angle and the components of the lever-arm, we can easily compute the lever-arm effects in other scenarios, which gives a thorough understanding of the effects resulted from various cases. Table 1 summaries the error statistics under all possible combinations. The upper portion tests the effect due to the presence of pitch only. The middle part examines the roll effect. The bottom one shows the results for general cases. From the table, we see that the noise level of the lever-arm error is extremely high if the lever-arm component is not along the rotation axis of the attitude angles. This is exactly what happened in the Alabama survey campaign whose lever-arm is $[\Delta x = -2.87\ \text{m}, \Delta y = 0.15\ \text{m}, \Delta z = 0.91\ \text{m}]^T$. The along track roll and pitch angles for Flight A are shown in Fig. 9. Beside the big jumps in the roll angle due to the turn of the aircraft around 7200 seconds, the attitude angles are generally small and smooth. However, the lever-arm errors as shown in Fig. 10 easily reach hundreds of mGals. Even after a 100-second window filtering, the errors (blue curves in Fig. 11) are still substantially large for any serious geodetic applications even when the RMS is indeed very small, 0.39 mGal. One has to increase the smoothing window to reduce the magnitude of the error if no accurate IMU attitude information is available. However, increasing the window size will not only reduce the spatial resolution of

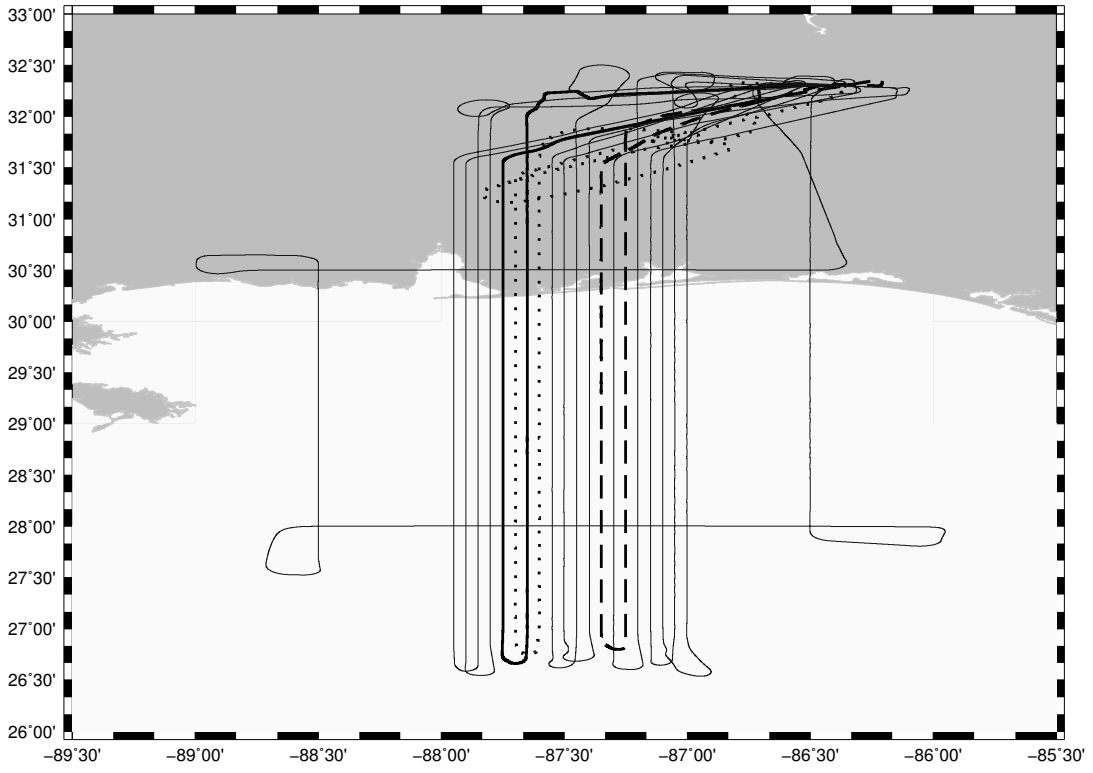

Figure 1. The Alabama aerogravity campaign conducted by NGS (Thicker lines, dotted lines, and dashed lines represent the trajectories of Flight A at 11 km high, Flight B at 6km high, and Flight C at 1.7 km high, respectively).

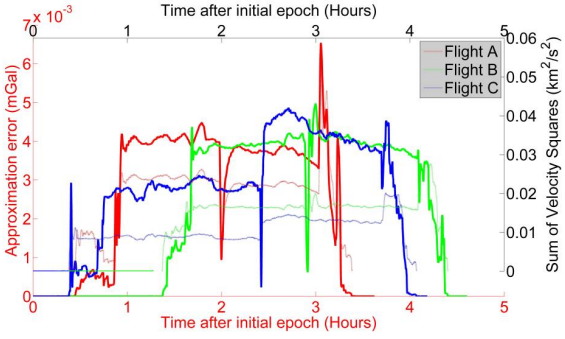

Figure 2. The approximation errors and their associated velocities along the entire selected flights. (The horizontal axes are unified at the corresponding initial epoch of each line.)

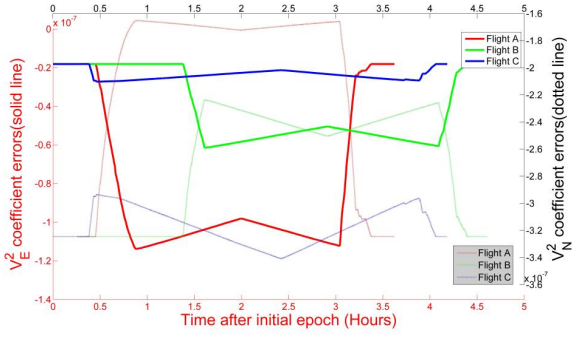

Figure 3. The approximation errors by neglecting the higher order terms (units are 1/m) in the coefficients of V_N^2 and V_E^2 in Eq. (1).

the data but also potentially under estimate the peak values of the gravity signal.

The next question that comes into mind is that under the perfect lever-arm setup, i.e. $\Delta x = 0$ m, $\Delta y = 0$ m, how accurate the attitude angles should be if one wants to do a perfect job and keep these errors in sub-mGal level in the raw gravity observations? To answer this question, we superpose certain amount of random noise on top of the real attitude angles that are shown in Figs 6-7.

The lever-arm effect differences due to these artificial random attitude errors for the case of the perfect setup ($[\Delta x = 0$ m, $\Delta y = 0$ m, $\Delta z = 1$ m$]^T$) are then computed. Table 2 gives the statistics corresponding to different noise levels, from which we can see that 10-arc-minute accuracy of the attitude angles is require for under 1 mGal noise and 5-arc-minute accurate attitude angles are needed if one wants to keep the raw errors under sub-mGal level so that no

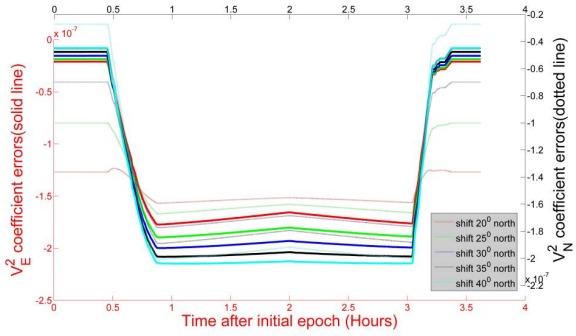

Figure 4. The approximation errors by neglecting the higher order terms (units are 1/m) in the coefficients of V_N^2 and V_E^2 in Eq. (1) along the simulated flights.

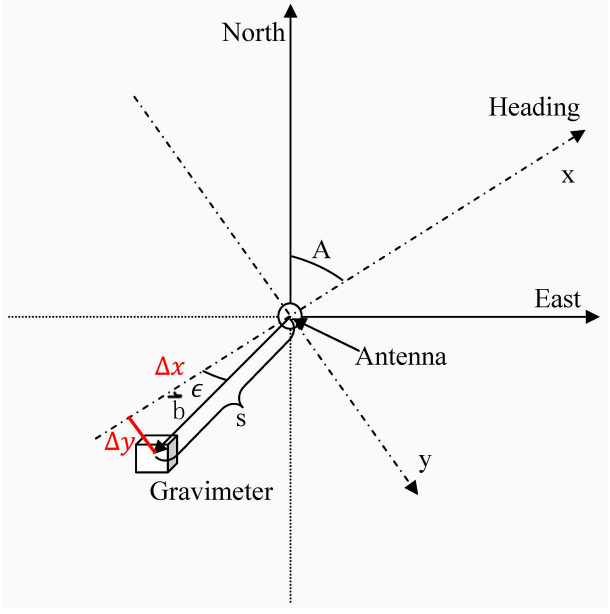

Figure 5. A diagram of the lever arm (the Down direction of navigation frame, indicated by the solid axes, and the z-axis of the b-frame (Jekeli 2000), indicated by the dashed axes, are pointing into the paper).

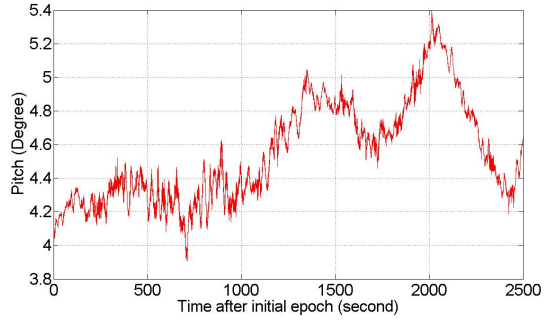

Figure 6. The IMU measured pitch angles along a typical flight.

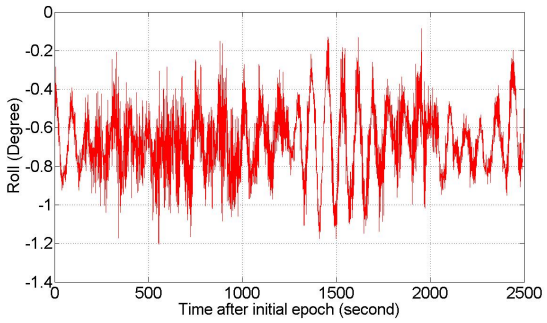

Figure 7. The IMU measured roll angles along a typical flight.

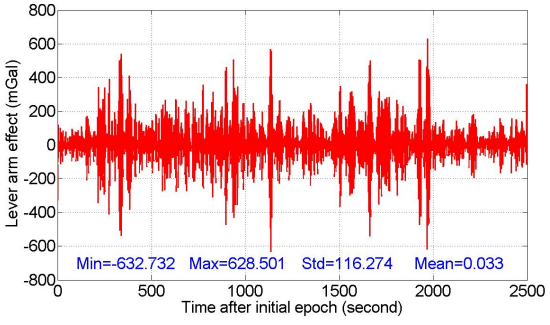

Figure 8. The simulated lever-arm effect.

more worries are needed for this issue in most of the mGal level or sub-mGal level accurate surveys.

4. Conclusions

The approximations in the Eötvös computation and lever-arm correction in the LCR based scalar gravimetric system are rigorously evaluated based on both simulated and real flight data sets. Numerical analysis shows that the magnitude of the higher order terms (not only the second order effect, but also the combination

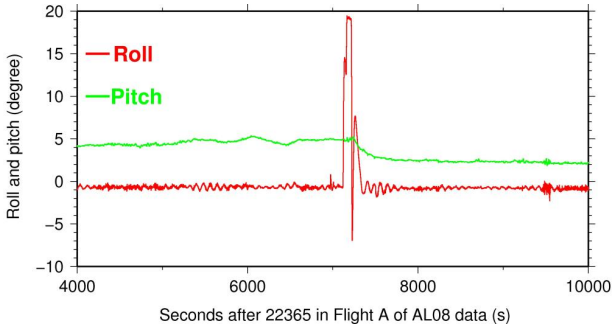

Figure 9. The attitude angles along the track of Flight A.

Table 1. The lever-arm simulation plans and their corresponding effects on the vertical acceleration. (The 0 and the 1 in the attitude columns represent their absence or appearance, respectively, in the simulation.)

roll	ptich	$\Delta x = 1$ (m)	$\Delta y = 1$ (m)	$\Delta z = 1$ (m)	Mean (mGal)	Std (mGal)	Min (mGal)	Max (mGal)
0	1	1	0	0	-0.019	20.421	-119.124	98.823
0	1	0	1	0	0.00	0.00	0.00	0.00
0	1	0	0	1	-0.001	1.617	-8.869	7.845
0	1	1	1	1	-0.020	22.035	-127.992	106.668
1	0	1	0	0	0.00	0.00	0.00	0.00
1	0	0	1	0	0.056	112.825	-993.303	995.482
1	0	0	0	1	0.001	1.385	-9.901	9.985
1	0	1	1	1	0.057	114.163	-993.443	992.693
1	1	1	0	0	-0.019	20.421	-119.124	98.823
1	1	0	1	0	0.048	111.832	-598.254	586.830
1	1	0	0	1	-0.001	2.187	-13.710	10.861
1	1	1	1	1	0.033	116.274	-632.732	628.501

Table 2. Attitude accuracy requirement analysis for lever-arm errors under perfect setup condition.

Added Noise roll	ptich	Mean mGal	Std mGal	Min mGal	Max mGal
0′	60′	0.002	0.278	-1.904	9.920
60′	0′	0.001	0.278	-1.143	4.597
60′	60′	0.001	0.390	-2.971	9.943
30′	30′	0.001	0.113	-0.743	5.612
10′	10′	0.000	0.012	-0.083	0.624
5′	5′	-0.000	0.003	-0.021	0.011
5″	5″	-0.137E-7	0.727E-6	-0.573E-5	0.314E-5

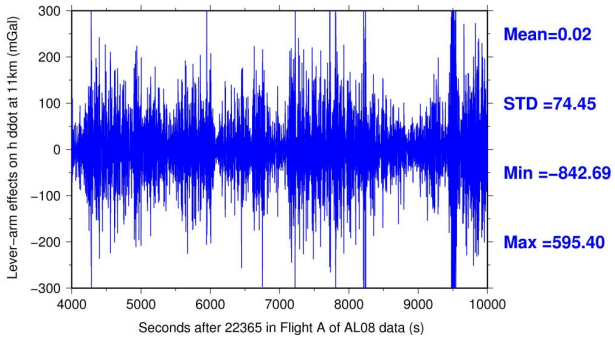

Figure 10. The lever-arm errors along the track of Flight A.

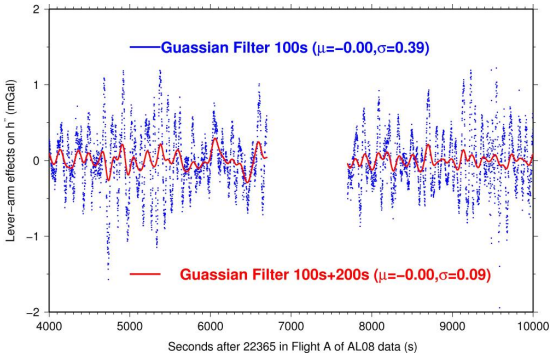

Figure 11. The filtered lever-arm errors along the track of Flight A.

effect of all high order terms) is indeed very small, at the μGal level. But it shows a systematic characteristic that is largely dependent on latitude and height. Thus, once the meter's observables are corrected into the local navigation frame, the exact formula such as given in Jekeli (2000) needs to be applied if one cannot tolerate these systematic effects or simply wants to avoid any arguments related to this issue.

With the on-board IMU provided attitude information, the lever-arm effects are also thoroughly analyzed. Simulation tests clearly show that the "horizontal" components of the lever-arm need to be kept as small as possible to avoid large (hundreds of mGals) errors. For real flights with poor lever-arm setup, large smoothing windows have to be applied if no accurate attitude information is available. However, this will definitely reduce the spatial resolution of

the gravity data. Even in the ideal lever-arm setup scenario, where no "horizontal offset" between the GPS antenna and the gravimeter is in presence, accurate (10 arc-minutes for mGal level and 5 arc-minutes for sub-mGal level) attitude information is required in order to totally remove the lever-arm induced noise that is in the accuracy range of most of the current airborne surveys. The benefit is that the wrong signal is directly removed from the raw gravity observables instead of by using various filters which are essentially stochastic tools whose result is always an estimate.

Appendix A: HARLAN'S APPROXIMATION

The exact formula for the kinematic vertical acceleration, $\vec{a} \cdot \vec{l}_z$, in the local frame, i.e., Eq. (4) in Harlan (1968), is repeated in Eq. (A1).

$$\begin{aligned} \vec{a} \cdot \vec{l}_z = \; & -\ddot{r}' \cos D + 2\dot{r}'\dot{D} \sin D \\ & + r'\dot{D}^2 \cos D + r'\ddot{D} \sin D \\ & - 2\dot{\phi}(\dot{r}' \sin D + r'\dot{D} \cos D) \\ & - r'\ddot{\phi} \sin D + \dot{\phi}^2(r' \cos D + h) \\ & + (\dot{l} + \omega_e)^2(r' \cos \phi \cos \phi_c + h \cos^2 \phi) \\ & - \ddot{h} \end{aligned} \tag{A1}$$

The approximated one, i.e., Eq. (13) in Harlan (1968), is also repeated here:

$$\begin{aligned} \vec{a} \cdot \vec{l}_z \cong \; & a\dot{\phi}^2 \left[1 + \tfrac{h}{a} + f(3 \sin^2 \phi - 2)\right] \\ & + a(\dot{l} + \omega_e)^2 \cos^2 \phi \\ & \times \left[1 + \tfrac{h}{a} + f \sin^2 \phi\right] - \ddot{h} \end{aligned} \tag{A2}$$

where $\vec{a}$ is the total kinematic acceleration; $\vec{l}_z$ is the unit vector along the vertical direction; a, b, and f are the semimajor axis, semiminor axis and flattening of the reference ellipsoid; ω_e is the mean Earth's angular rotation rate; r' is the distance from the center of the reference ellipsoid to the aircraft's corresponding point, p, on the surface of the reference ellipsoid; h and $\ddot{h}$ are the ellipsoid height of the aircraft and its second derivatives with respect to time; ϕ_c and ϕ are the geocentric and geodetic latitudes and D is their angular deviation along the normal of the surface of the reference ellipsoid at point p (all their overhead dot/dots are for the first or second order derivatives with respect to time); and $\dot{l}$ is the longitude derivative with respect to time.

References

Brozena J.M. and Peters M.F., 1988, An airborne gravity study of eastern North Carolina, Geop., 53, 2, 245-253.

de Saint-Jean B., Verdun J., Duquenne H., Barriot J.P., Melachroinos S. and Cali J., 2007, Fine analysis of lever arm effects in moving gravimetry. In: Tregoning P and Rizos C, (eds.), Proc. of Dynamic Planet - Monitoring and Understanding a Dynamic Planet with Geodetic and Oceanographic Tools, volume 130 of IAG Symposia, pages 809-816, Cairns, Australia.

Forsberg R., Olesen A.V., Keller K. and Moller M., 2001, Airborne gravity and geoid surveys in the Arctic and Baltic seas, Proc., Int. Sym. on Kinematic Systems in Geodesy, Geom. and Navi., Banff, Canada, pp 586-593.

Harlan R.B., 1968, Eötvös correction for airborne gravimetry, J. Geop. Res., 73, 14, 4675-4679.

Heiskanen W.A., and Moritz H., 1967, Physical Geodesy. W.H. Freeman and Company, San Francisco, California and London.

Jekeli C., 2000, Inertial Navigation Systems with Geodetic Applications, W. deGruyter, Berlin, 2000.

Kwon J.H. and Jekeli C., 2001, A new approach for airborne vector gravimetry using GPS/INS, J Geod., 74, 10, 690-700.

Li X., 2007, Moving base INS/GPS vector gravimetry on a land vehicle. PhD dissertation, OSU report 486.

Li X. and Jekeli C., 2008, Ground-Vehicle INS/GPS Gravimetry, Geop., 73, 2, I1-I10.

Li X., 2011a, Strapdown INS/DGPS airborne gravimetry tests in the Gulf of Mexico, J Geod., 85, 9, 597-605, DOI: 10.1007/s00190-011-0462-2.

Li X., 2011b, An Exact Formula for the Tilt Correction in Scalar Airborne Gravimetry, J Appl. Geod., 5, 2, 81-85, DOI: 10.1515/JAG.2011.007.

Melachroinos S.A., Tchalla M., Biancale R. and Menard Y., 2010, Removing attitude-related variations in the line-of-sight for kinematic GPS positioning, GPS Solu., 15, 3, 275-285.

Olesen A.V., 2003, Improved Airborne Scalar Gravimetry for Regional Gravity Field Mapping and Geoid Determination. Technical Report no 24, Kort og Matrikels Styrelsen, Copenhagen.

Rummel R., 1979, Determination of short-wavelength components of the gravity field from satellite-to-satellite tracking or satellite gradiometry-an attempt to an identification of problem areas, Manu. Geod. 4, 2, 107-148.

Sander L. and Ferguson S., 2010, Advances in SGL AIRGrav acquisition and processing, ASEG (Australian Society of Exploration Geophysicists) Conference, Sydney, Australia.

Sander S., Sander L. and Ferguson S., 2011, SGL AIRGrav Anomaly Detection from Modeling and Field Data using Advanced Acquisition and Processing, Sander Geophysics, GEM (International Workshop on Gravity, Electrical and Magnetic Methods), Beijing, China.

Smith D.A., 2007, The GRAV-D Project: Gravity for the Redefinition of the American Vertical Datum, NOAA/National Geodetic Survey: http://www.ngs.noaa.gov/grav-d/pubs/GRAV-D_v2007_12_19.pdf (accessible by Oct 2011).

Studinger M., Bell R. and Frearson N., 2008, Comparison of AIRGrav and GT-1A airborne gravimeters for research applications. Geop., 73, 6, 151-161.

Valliant H., 1992, The LaCoste & Romberg air/sea gravimeter: an overview: In: CRC Handbook of Geophysical Exploration at Sea, 2nd Edition, Volume 1, 141-176. Boca Raton Press.

Verdun J., 2000, La gravimétrie aéroportée en région montagneuse; Exemple de levé franco-suisse sur les Alpes Occidentales. Thése pour obtenir le grade de Docteur de Université Montpellier II, France

Wahr J., 1996, Geodesy and Gravity. Department of Physics, University of Colorado, Boulder, CO, Samizdat Press.